



## SYNTHESIS, CHARACTERIZATION AND CATALYTIC PERFORMANCE OF CERIA-SUPPORTED COBALT CATALYST FOR METHANE DRY REFORMING TO SYNGAS

(Sintesis, Pencirian dan Prestasi Mangkin Kobalt Sokongan Ceria untuk Penghasilan Semula Metana Kontang Kepada Gas Sintesis)

Bamidele V. Ayodele<sup>1,2</sup>, Mohd Nasir Nor Shahirah<sup>1,2</sup>, Maksudur R. Khan<sup>1</sup>, Chin Kui Cheng<sup>1,2\*</sup>

<sup>1</sup>Faculty of Chemical & Natural Resources Engineering

<sup>2</sup>Centre of Excellence for Advanced Research in Fluid Flow (CARIFF)

Universiti Malaysia Pahang, Lebuhraya Tun Razak, 26300 Gambang Kuantan, Malaysia

\*Corresponding author: [chinkui@ump.edu.my](mailto:chinkui@ump.edu.my)

Received: 21 October 2015; Accepted: 14 June 2016

### Abstract

In this study the synthesis, characterization and catalytic performance of CeO<sub>2</sub> (Ceria) supported Co catalyst was investigated. First, the ceria was synthesized by direct thermal decomposition of Ce(NO<sub>3</sub>)<sub>3</sub>·6H<sub>2</sub>O and subsequently impregnated with 20 wt.% Co using aqueous solution of Co(NO<sub>3</sub>)<sub>2</sub>·6H<sub>2</sub>O as a precursor. The synthesized catalyst was characterized using TGA, N<sub>2</sub>-adsorption-desorption, X-ray Diffractometry (XRD), Field Emission Scanning Electron Microscope (FESEM-EDX), and Fourier Transformation Infrared (FTIR). The catalytic property of the ceria-supported cobalt catalyst was tested in methane dry reforming using a stainless steel fixed bed reactor. The dry reforming reaction was performed at the temperature range of 923-1023 K under a controlled atmospheric pressure and constant gas hourly space velocity (GHSV) of 30000 h<sup>-1</sup>. The effects of reactant (CH<sub>4</sub> and CO<sub>2</sub>) feed ratio was investigated on reactants conversion, product yields, and selectivity. The ceria-supported cobalt catalyst recorded highest catalytic activity at a CH<sub>4</sub>: CO<sub>2</sub> ratio of 0.9 and temperature of 1023 K. The highest values of 79.5% and 87.6% were recorded for the CH<sub>4</sub> and CO<sub>2</sub> conversions respectively. Furthermore, highest yields of 41.98% and 39.76%, as well as selectivity of 19.56% and 20.72%, were obtained for H<sub>2</sub> and CO respectively. Syngas ratio of 0.90 was obtained from the dry reforming of methane, making it suitable as feedstock for Fischer-Tropsch synthesis (FTS).

**Keywords:** ceria, cobalt, Fischer-Trosch synthesis, methane dry reforming, syngas

### Abstrak

Dalam kajian ini, sintesis, pencirian berserta prestasi tindakbalas pemangkin Co/CeO<sub>2</sub> telah dijalankan. Terdahulu, ceria disintesis daripada penguraian terma secara langsung ke atas Ce(NO<sub>3</sub>)<sub>3</sub>·6H<sub>2</sub>O, diikuti oleh formulasi dengan 20% logam Co menggunakan larutan akueus Co(NO<sub>3</sub>)<sub>2</sub>·6H<sub>2</sub>O sebagai pelopor. Mangkin yang diperolehi dicirikan dengan menggunakan kaedah TGA, N<sub>2</sub>-penjerapan penyaherapan, pembelauan sinar X (XRD), Mikroskop Pengimbas Elektron Pancaran Medan – Sinar-X Serakan Tenaga (FESEM-EDX) dan Inframerah Tranformasi Fourier (FTIR). Prestasi pemangkin Co/CeO<sub>2</sub> telah diuji untuk tindakbalas penghasilan metana kontang di dalam reaktor keluli tahan karat. Tindakbalas kimia tersebut telah dijalankan pada suhu berjalut daripada 923-1023 K, tekanan 1 atm serta GHSV bersamaan 30000 h<sup>-1</sup>. Kesan nisbah reaktan (CH<sub>4</sub> and CO<sub>2</sub>) terhadap penukaran reaktan serta hasil dan pemilihan produk telah disiasat. Mangkin Co/CeO<sub>2</sub> mencatatkan aktiviti pemangkin paling tinggi pada nisbah CH<sub>4</sub>/CO<sub>2</sub> bersamaan 0.9 dan suhu 1023 K. Penukaran CH<sub>4</sub> and CO<sub>2</sub> mencatatkan nilai tertinggi bersamaan 79.5% dan 87.6%. Tambahan pula, hasil tertinggi bersamaan 37.6% dan 40% berserta sifat pemilihan bersamaan 19.56% dan 20.72% untuk H<sub>2</sub> dan CO telah direkodkan. Nisbah gas sintesis bersamaan 0.9 telah diperolehi daripada penghasilan semula metana kontang bersesuaian untuk tindakbalas sintesis Fischer-Trosch.

**Kata kunci:** ceria, kobalt, sintesis Fischer-Tropsch, penghasilan semula metana, gas sintesis

### Introduction

The utilization of energy derived from fossil sources as transportation fuel has been one of the major concerns of researchers in the past five decades [1,2]. This is due to the emissions of greenhouse gases such as CO<sub>2</sub> into the biosphere during the combustion of these fuels [3,4]. Several reports have shown that these greenhouse gases are the main causes of global warming through “greenhouse effect” [5–7]. Efforts of researchers have been concentrated on how to mitigate the emissions of these greenhouse gases [3,8,9]. Methane (CH<sub>4</sub>) is one of the key components of greenhouse gases as well as a major source of fossil fuel [10]. It is inexpensive and abundance in nature, hence a good building block for C<sub>1</sub> chemistry [11]. One way to mitigate the emissions of the greenhouse gases, as well as increasing energy output via dry reforming process [9].

Dry reforming of methane depicted in Equation (1) has received wide research attention due to its advantage to utilize both CO<sub>2</sub> and CH<sub>4</sub>, the two principal components of greenhouse gases for production of synthesis gas (a mixture of H<sub>2</sub> and CO) [12–14]. This syngas can be used as chemical intermediates for the production of synthetic fuel via Fischer-Tropsch synthesis (FTS) [15,16].



Dry reforming of methane as a highly endothermic process is majorly constraint with catalyst deactivation from sintering and carbon deposition [17,18]. There have been concerted efforts by researchers in the field of catalysis in designing and developing catalysts with high activity and stability to overcome challenges of sintering and carbon depositions [19,20].

Up to date, the activity and stability of supported metal-based catalysts such as Pt, Pd, Ru, Rh, Ir, Ni and Co, have been investigated for dry reforming of methane [21]. Reports have shown that supported noble metals catalysts such as Pt, Pd, Ru, Rh, and Ir are very active and highly stable during dry reforming of methane [22–24]. However, these noble-metal catalysts are not readily available and very expensive [25]. Hence, the application of these noble metals to catalyze dry reforming of methane will not be economical in the event of scale up. Supported Ni-based catalysts have high activity and are inexpensive [26]. Nevertheless, the usage of Ni-based catalysts in dry reforming of methane has been constraint by their susceptibility to catalyst deactivation via sintering and carbon depositions [27]. Supported Co-catalyst which is less expensive compared to noble-metal catalysts has been reported as a good alternative to Ni-based catalysts in terms of stability [28].

In addition to using good metal-based catalysts, its play a significant role in enhancing the thermal stability of catalysts during dry reforming of methane [29]. Reports have shown that efficient dispersion of active metals on supports such as SiO<sub>2</sub>, α-Al<sub>2</sub>O<sub>3</sub>, CeO<sub>2</sub>, La<sub>2</sub>O<sub>3</sub> and ZrO<sub>2</sub> to a large extent affect the pore morphology, confinement and chemical effect of the catalysts [30]; [14]. This will invariably retard coke formation as well as reduce the tendency of the active metal to sinter. The use of ceria (CeO<sub>2</sub>)-supported Co catalyst has been extensively studied for ethanol steam reforming [31–33]. However, there are limited studies on the dry reforming of methane over ceria supported Co catalyst [34, 35].

This present study focuses on the synthesis, characterization and catalytic performance of ceria supported Co catalyst for dry reforming of methane. The ceria support was prepared by thermal decomposition of cerium (III) nitrate hexahydrate and subsequently used for the synthesis of the Co/CeO<sub>2</sub> catalyst via wet impregnation method [36].

### Materials and Methods

#### Catalyst synthesis

The schematic diagram depicting the steps involved in the catalyst synthesis is shown in Figure 1. First, the ceria support used for the catalyst synthesis was prepared by thermal decomposition of Ce(NO<sub>3</sub>)<sub>3</sub>·6H<sub>2</sub>O (99.99% trace metal basis, Sigma-Aldrich) at 773 K for 2 hours to obtained CeO<sub>2</sub> powder [36,37]. The CeO<sub>2</sub> powder was

subsequently impregnated with aqueous solution of  $\text{Co}(\text{NO}_3)_2 \cdot 6\text{H}_2\text{O}$  (20 wt% Co loading) by wet impregnation method and then stirred continuously for 3 hours at room temperature. Thereafter, the mixture containing the catalyst precursor and the support was dried at 393 K for 24 hours and then calcinate at 873 K for 5 hours.

### Catalyst characterization

The physicochemical properties of the fresh 20 wt% Co/CeO<sub>2</sub> catalyst were determined by temperature programmed calcination using thermogravimetric analyzer (TA instrument, Q 500). The catalyst sample was heated from 298 to 1173 K at heating rates of 10, 15 and 20 K/min. The specific surface area, pore volume and average pore diameter of the catalyst were measured by N<sub>2</sub> adsorption-desorption isotherm at 77 K using Thermo Scientific Surfer Analyzer. Prior to the N<sub>2</sub> adsorption-desorption experiment, the catalyst was degassed at 573 K for 3 hours. Phase identification, as well as the crystallinity of the 20 wt% Co/CeO<sub>2</sub> catalyst, was determined by Rigaku X-ray powder diffraction analysis (XRD) (Miniflex II) with Cu K $\alpha$  (45kV, 0.154 nm) radiation.

The morphology and elemental composition of the catalyst sample were carried out using JEOL FESEM (JSM-7800F) equipped with EDX. Temperature-programmed reduction (TPR) of the fresh catalyst was performed in a fixed bed reactor. The catalyst weighing 200 mg was heated from 373 – 1073 K in a flow of 60 ml/min of H<sub>2</sub>/N<sub>2</sub> (1:5). The amount of hydrogen consumed was measured using gas chromatography (GC) equipped with thermal conductivity detector (TCD). The GC consists of two packed columns namely Supelco Molecular Sieve 13x (10 ft  $\times$  1/8 in OD  $\times$  2 mm ID, 60/80 mesh, Stainless Steel) and Agilent Hayesep DB (30 ft  $\times$  1/8 in OD  $\times$  2 mm ID, 100/120 mesh, Stainless Steel). Helium gas with flow rate of 20 ml min<sup>-1</sup> was used as the carrier at operating column temperature of 393 K.

The nature of chemical bond of the catalyst was measured using Perkin Elmer Fourier transform infrared (FTIR) (Nicolet iS-50) spectrometer. The sample was analysed using an attenuated total reflectance (ATR) method within 4000-400 cm<sup>-1</sup>.

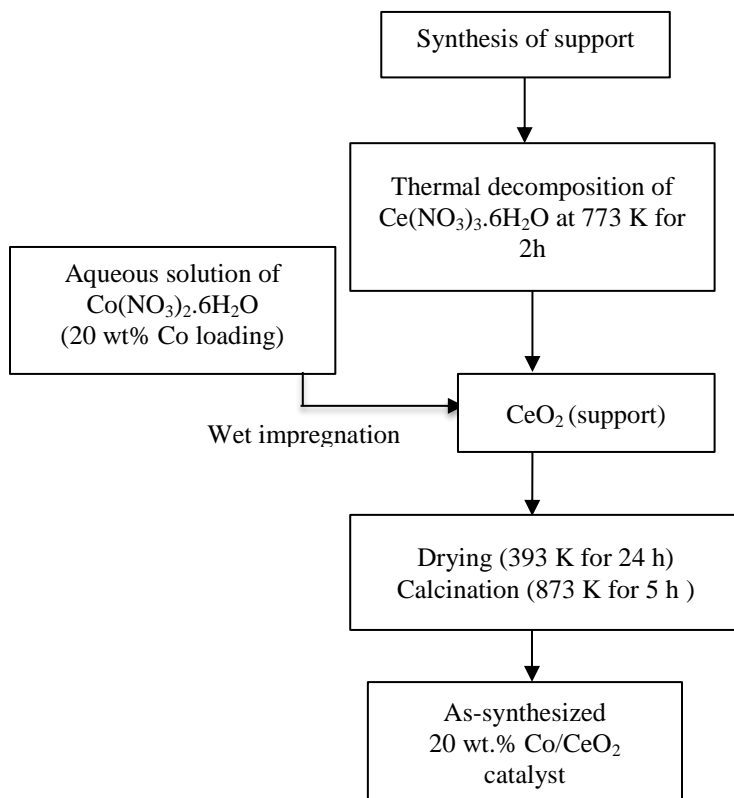


Figure 1. Schematic diagram of steps involved in the synthesis of the 20 wt% Co/CeO<sub>2</sub> catalyst

### Catalyst activity test

The catalyst activity test was performed in a stainless steel fixed bed reactor under controlled atmospheric pressure. The stainless steel tubular reactor was loaded with 200 mg catalyst sample supported with quartz wool. The fixed bed reactor was positioned in a furnace equipped with a Type-K thermocouple to monitor the temperature of the catalytic bed. Prior to the commencement of the activity test, the catalyst was reduced *in situ* in a flow of 60 ml/min of H<sub>2</sub>/N<sub>2</sub> (1:5) at 873 K for 1 h. The flow of the reactant gases (CH<sub>4</sub> and CO<sub>2</sub>) into the reactor was monitored using Alicat digital mass flow controller. The dry reforming of methane was performed at varying feed ratios ranged 0.1-1.0 and reaction temperature ranged 923 – 1023 K. The compositions of the reactant gases as well as the products (H<sub>2</sub> and CO) were monitored using GC-TCD. The activity of the catalyst was measured based on the conversions of the reactants, the yield, and selectivity of the products formed as shown in equations (2) – (7).

$$\text{CH}_4 \text{ conversion (\%)} = \frac{F_{\text{CH}_4\text{in}} - F_{\text{CH}_4\text{out}}}{F_{\text{CH}_4\text{in}}} \times 100 \quad (2)$$

$$\text{CO}_2 \text{ conversion (\%)} = \frac{F_{\text{CO}_2\text{in}} - F_{\text{CO}_2\text{out}}}{F_{\text{CO}_2\text{in}}} \times 100 \quad (3)$$

$$\text{H}_2 \text{ yield} = \frac{F_{\text{H}_2\text{out}}}{2 \times F_{\text{CH}_4\text{in}}} \times 100 \quad (4)$$

$$\text{CO yield} = \frac{F_{\text{COout}}}{F_{\text{CH}_4\text{in}} + F_{\text{CO}_2\text{in}}} \times 100 \quad (5)$$

$$\text{H}_2 \text{ Selectivity} = \frac{F_{\text{H}_2\text{out}}}{F_{\text{H}_2\text{out}} + F_{\text{CH}_4\text{out}} + F_{\text{CO}_2\text{out}} + F_{\text{CO}}} \times 100 \quad (6)$$

$$\text{CO Selectivity} = \frac{F_{\text{COout}}}{F_{\text{CH}_4\text{out}} + F_{\text{CO}_2\text{out}} + F_{\text{COout}}} \times 100 \quad (7)$$

$F_{\text{CO}_2\text{in}}$  = inlet molar flow of CO<sub>2</sub>;  $F_{\text{CO}_2\text{out}}$  = outlet molar flow of CO<sub>2</sub>;  $F_{\text{CH}_4\text{in}}$  = inlet molar flow of CH<sub>4</sub>;  $F_{\text{CH}_4\text{out}}$  = outlet molar flow of CH<sub>4</sub>;  $F_{\text{H}_2\text{out}}$  = outlet molar flow of H<sub>2</sub>;  $F_{\text{COout}}$  = outlet molar flow of CO.

## Results and Discussion

### Catalyst characterization

The temperature programmed calcination of the fresh catalyst is shown in Figure 2. Four distinct peaks (I to IV) can be identified from the TGA curve. Peaks I-III can be attributed to sequential loss of physical and hydrated water while peak IV depicts decomposition of the cobalt nitrate to obtain Co<sub>3</sub>O<sub>4</sub>. This trend is consistent with the findings of [38] in their study on dry reforming of methane over alumina supported cobalt catalyst.

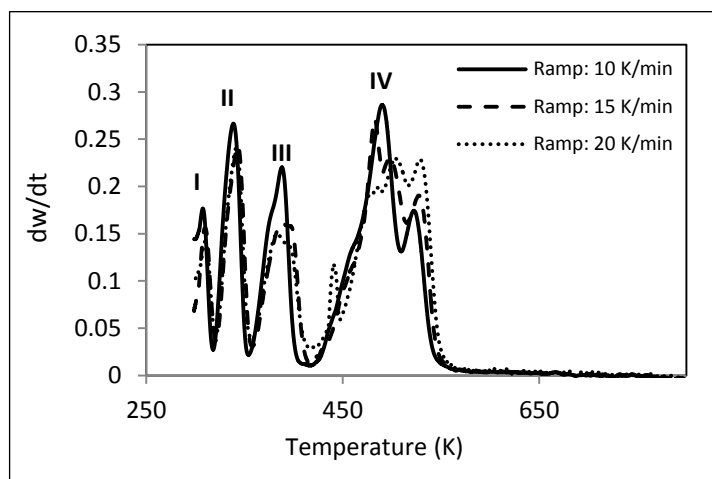


Figure 2. Temperature Programmed Calcination of the 20 wt% Co/CeO<sub>2</sub> catalyst

The determination of the mesoporous structure and specific surface of the 20 wt% Co/CeO<sub>2</sub> catalyst from N<sub>2</sub> adsorption-desorption isotherm is depicted in Figure 3. The Co/CeO<sub>2</sub> catalyst isotherm has a characteristic of Type IV isotherm curve with H3 hysteresis loop. Since the relative pressure ( $P/P^0$ ) is  $> 0.55$ , the catalyst exhibited uniform mesoporous structure with capillary condensation. The BET specific area of the catalyst was estimated from the sorptomatic data processing software as 39.89 m<sup>2</sup>g<sup>-1</sup> while the pore volume and average pore diameter obtained from Barrett, Joyner, and Hallenda (BJH) method were estimated to be 0.0141 cm<sup>3</sup>g<sup>-1</sup>, and 1.16 nm respectively.

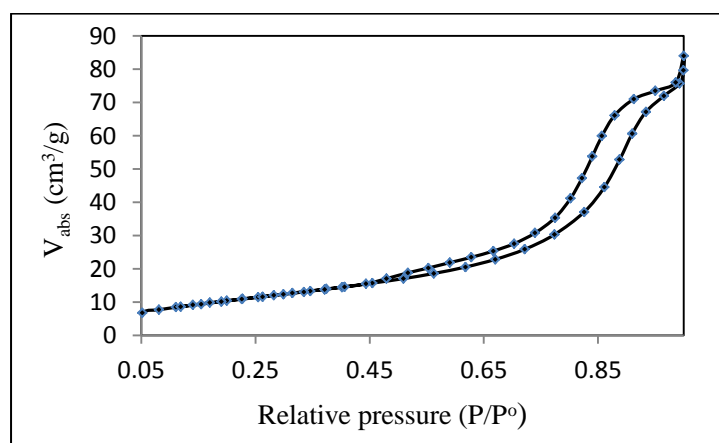


Figure 3. N<sub>2</sub> adsorption-desorption isotherm of the 20 wt% Co/CeO<sub>2</sub> catalyst

The XRD pattern of the catalyst sample is depicted in Figure 4. Distinct peaks of CeO<sub>2</sub> and Co<sub>3</sub>O<sub>4</sub> crystals can be seen at  $2\theta = 29.4^\circ, 38.4^\circ, 48.7^\circ, 57.9^\circ$  and  $2\theta = 31.3^\circ, 44.5^\circ, 59.7^\circ, 65.1^\circ, 67.7^\circ, 77.1^\circ$  respectively. The diffraction peaks obtained for CeO<sub>2</sub> can be assigned to the crystalline phase of (111), (220), (311), (220) and (422) which represent faced-centre cubic structure [39].

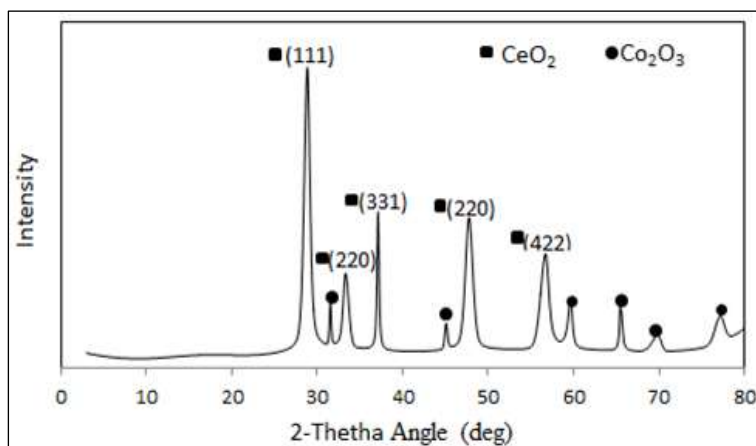


Figure 4. XRD pattern of the 20 wt% Co/CeO<sub>2</sub> catalyst

The FESEM micrograph and EDX dot mapping showing the morphology and the elemental composition of the 20 wt% Co/CeO<sub>2</sub> catalyst are depicted in Figures 5-7 respectively. The FESEM micrograph (Figure 5) shows the

irregularity and the agglomeration of the catalyst particle sizes. While the EDX dot mapping (Figure 6) confirms the presence of Co, Ce and O as stimulated during the synthesis of the catalyst. The elemental compositions of the catalysts obtained from the EDX dot mapping (Figure 7) corresponds to the stimulated amount used for the catalysts synthesis.

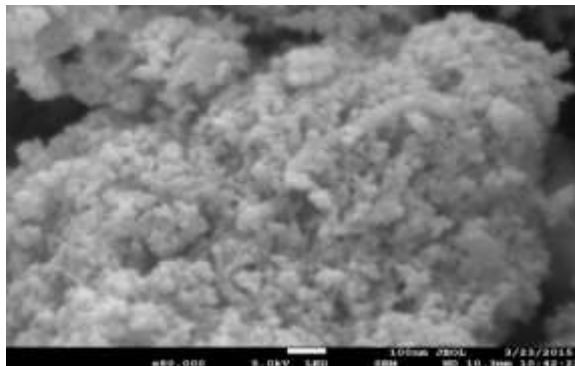


Figure 5. The FESEM micrograph of the 20 wt% Co/CeO<sub>2</sub> catalyst

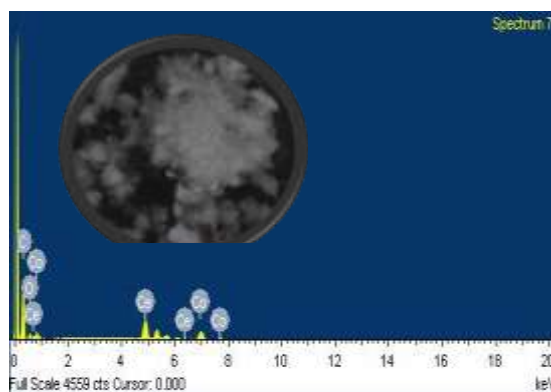


Figure 6. The EDX dot mapping of the 20 wt% Co/CeO<sub>2</sub> catalyst

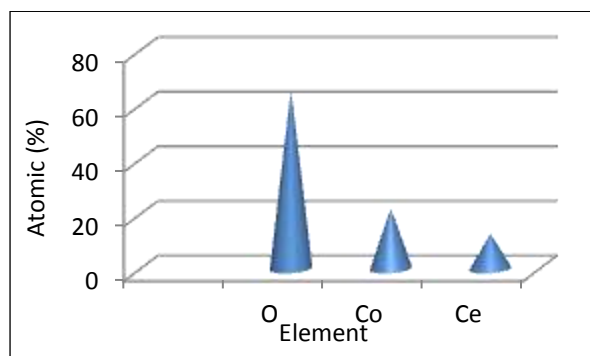


Figure 7. The elemental composition of the 20 wt% Co/CeO<sub>2</sub> catalyst obtained from EDX-mapping

In order to check the reducibility of the catalyst in a flow of H<sub>2</sub>, the catalyst was subjected to H<sub>2</sub>-TPR. Significantly, two peaks centralized at a temperature of 423, and 673 K can be identified from the H<sub>2</sub>-TPR profile. The peaks could be attributed to the sequential reduction of Co<sub>3</sub>O<sub>4</sub> to Co crystallite represented in equation 8. The peak at 423 K could be attributed to the reduction of Co<sub>3</sub>O<sub>4</sub> which has a weak interaction with the support to CoO. The peak at 577K with a stronger interaction can be attributed to the reduction of CoO to Co [40].

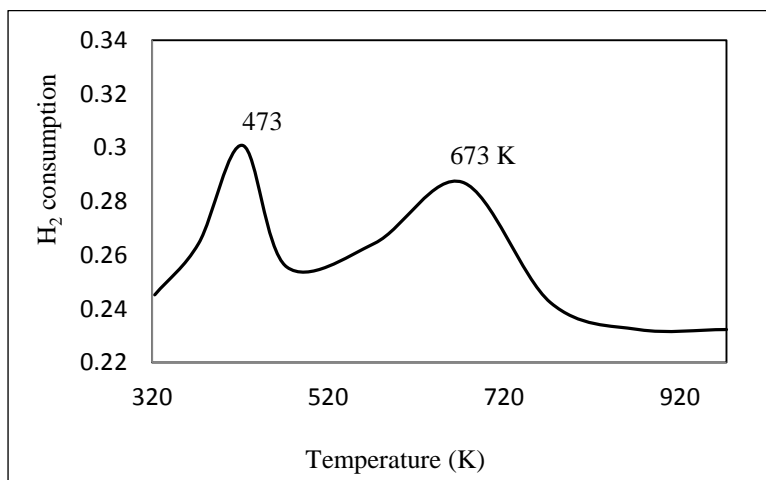
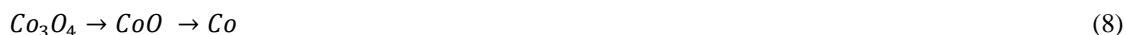


Figure 8. H<sub>2</sub>-TRP profile of the 20 wt% Co/CeO<sub>2</sub> catalyst

The FTIR spectra of the catalyst are shown in Figure 9. The spectra band can be identified at 3400, 1670, 667 and 567 cm<sup>-1</sup> respectively. The bands at 3400 and 1670 cm<sup>-1</sup> can be attributed to OH<sup>-</sup> which is due to water moisture and COO from dissolved atmospheric CO<sub>2</sub>. The band obtained at 1670 and 667 cm<sup>-1</sup> can be attributed to stretching metal oxides (M-O) bond from Co-O and Ce-O respectively.

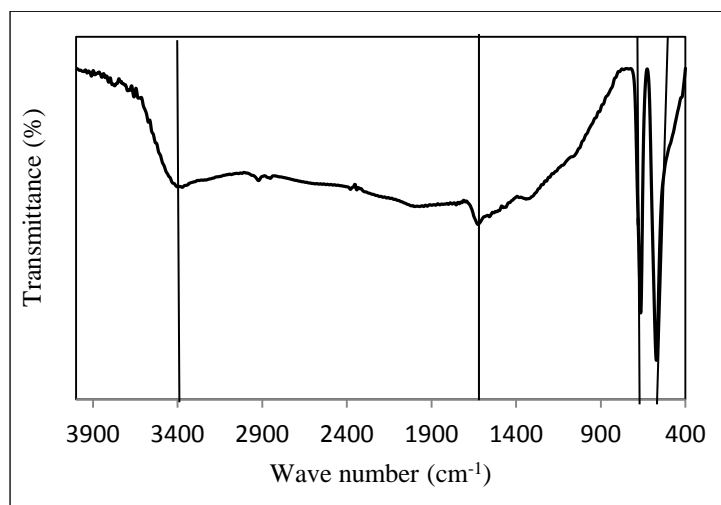


Figure 9. FTIR spectra of the 20 wt% Co/CeO<sub>2</sub> catalyst

### Catalyst activity

The performance of the ceria supported Co catalyst was measured from the conversions of the reactant gas to syngas, the yields of the syngas produced as well as the products selectivity. The effects of feed ratios (0.1-1.0) and temperature (923 – 1023K) were investigated on the catalyst activity in terms of conversions, yields, and selectivity in methane dry reforming process. The conversions of CH<sub>4</sub> and CO<sub>2</sub> depicted in Figures 10 and 11 increases with feed ratio and temperature signifying the temperature dependent nature of the dry reforming reaction. The conversion of CH<sub>4</sub> increases from 43.2% to a maximum value of 79.5%. Similarly, conversion of CO<sub>2</sub> increases from 17.8% to 87.6%. The catalyst shows higher activity towards CO<sub>2</sub> conversion compared to CH<sub>4</sub>. This could be as a result of reversed water gas shift reaction shown in equation 9 [41].

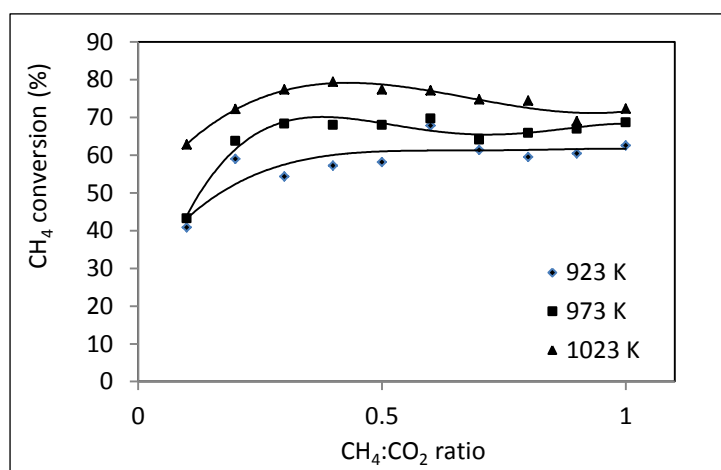


Figure 10. Effect of feed ratio and temperature on conversion of CH<sub>4</sub> over 20 wt% Co/CeO<sub>2</sub> catalyst

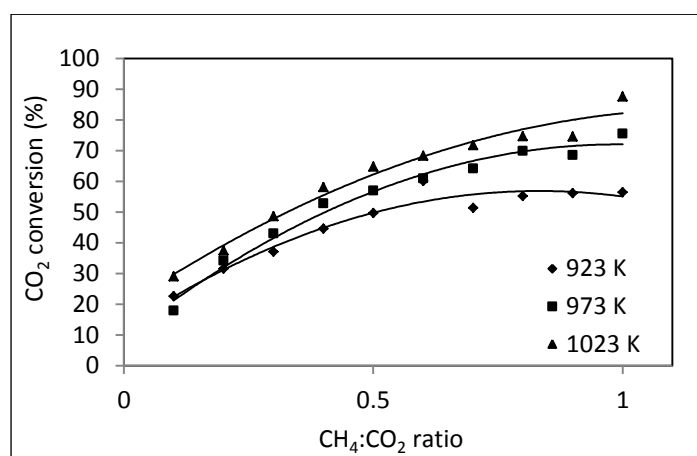


Figure 11. Effect of feed ratio and temperature on conversion of CO<sub>2</sub> over 20 wt% Co/CeO<sub>2</sub> catalyst.



The catalytic performances of the 20 wt% Co/CeO<sub>2</sub> catalyst in term of products (CO and H<sub>2</sub>) yields are depicted in Figures 12 and 13, respectively. It is noteworthy that both H<sub>2</sub> and CO yields increase with feed ratios and temperature. The yield of H<sub>2</sub> increases from 1.69% to reach a maximum value of 41.98%. While the yield of CO increases from 6.56% to the maximum value of 39.76%. A similar observation has been reported by Sajjidi et al. [42] for dry reforming of methane over Ni-Co/Al<sub>2</sub>O<sub>3</sub>-ZrO<sub>2</sub> nanocatalyst. The highest yield of 42% and 58% were obtained for H<sub>2</sub> and CO respectively. In the present study, at the highest yield of H<sub>2</sub> and CO, syngas ratio of 1.05 was obtained. This makes the syngas produced from the dry reforming of methane over the 20 wt% Co/CeO<sub>2</sub> catalyst suitable as a chemical intermediate to produce oxygenated fuel via FTS. Apparently, the catalyst shows a higher activity towards H<sub>2</sub> yield compared to CO yield. The observation could be attributed to temperature dependent nature of CH<sub>4</sub> decomposition. The decomposition of CH<sub>4</sub> increases with temperature leading to an increase in the formation of H<sub>2</sub> [43].

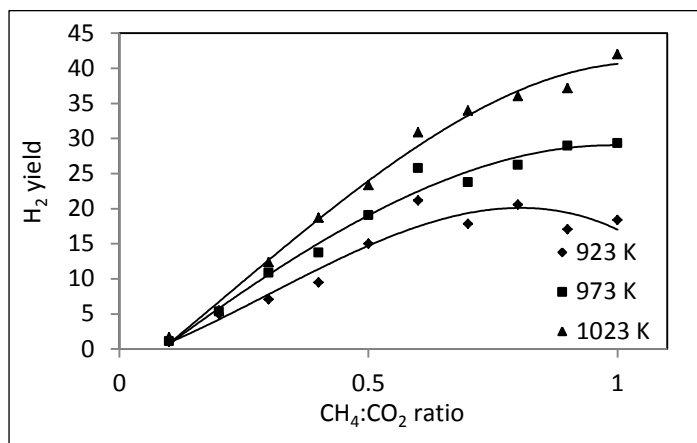


Figure 12. Effect of feed ratio and temperature on the yield of H<sub>2</sub> over 20 wt% Co/CeO<sub>2</sub> catalyst

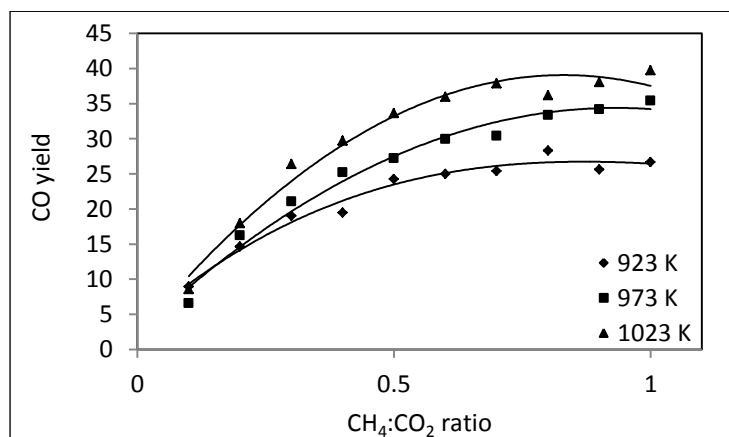


Figure 13. Effect of feed ratio and temperature on the yield of CO over 20 wt% Co/CeO<sub>2</sub> catalyst

The selectivity of the 20 wt% Co/CeO<sub>2</sub> catalyst towards H<sub>2</sub> and CO production is shown Figures 14 and 15, respectively. The H<sub>2</sub> and CO selectivity significantly increase with feed ratio and temperature from 1.16% and 8.56% to reach a maximum value of 19.56% and 20.72% respectively. This observation is consistent with the findings of Zheng et al. [44] who employed Co/ $\gamma$ -Al<sub>2</sub>O<sub>3</sub> for dry reforming of methane to syngas. The authors,

however, obtain a higher selectivity of 95% and 85% for H<sub>2</sub> and CO. The difference in result could be linked to high surface area  $\gamma$ -Al<sub>2</sub>O<sub>3</sub> used as support compared to Ceria as well as the difference in experimental conditions.

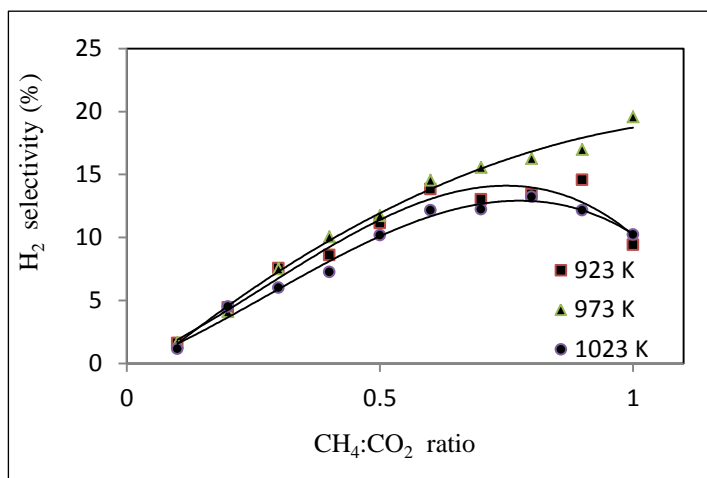


Figure 14. Effect of feed ratio and temperature on the selectivity of H<sub>2</sub> over 20 wt% Co/CeO<sub>2</sub> catalyst

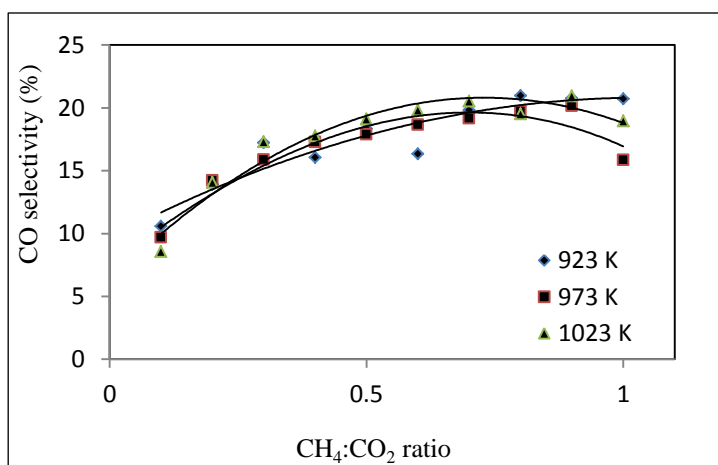


Figure 15. Effect of feed ratio and temperature on the selectivity of CO over 20 wt% Co/CeO<sub>2</sub> catalyst

### Conclusion

In this study, we have reported the synthesis, characterization and catalytic performance of ceria supported Co catalyst. The catalyst was synthesized by wet impregnation method and characterized by different physicochemical properties using techniques such as TGA, N<sub>2</sub>-adsorption-desorption, XRD, FESEM-EDX, and FTIR. The catalytic performance of the as-synthesized catalyst was tested in dry reforming of methane for the production of syngas. The catalyst shows good performance towards reactant conversion, products yield, and selectivity. Syngas ratio of 0.9 was produced from the dry reforming of methane over the ceria supported catalyst, making the process suitable for the production of feedstock for FTS process.

### Acknowledgement

The authors would like to acknowledge the research fund RDU130501 granted by the Ministry of Science, Technology and Innovation Malaysia (MOSTI) and the DSS scholarship granted to Bamidele V. Ayodele by Universiti Malaysia Pahang.

### References

- Guo, S., Shao, L., Chen, H., Li, Z., Liu, J. B., Xu, F. X., Li, J. S., Han, M. Y., Meng, J., Chen, Z. M. and Li, S. C. (2007). Inventory and input-output analysis of CO<sub>2</sub> emissions by fossil fuel consumption in Beijing. *Ecological Informatics*, 12: 93 – 100.
- Shearer, C., Bistline, J., Inman, M. and Davis, S. J. (2014). The effect of natural gas supply on US renewable energy and CO<sub>2</sub> emissions. *Environmental Research Letters*, 9(9): 1 - 12.
- Clarke, L., Kyle, P., Wise, M., Calvin, K., Edmonds, J., Kim, S., Placet, M. and Smith, S. (2008). CO<sub>2</sub> Emissions mitigation and technological advance : An updated analysis of advanced technology scenarios *PNNL Report Pacific Northwest National Laboratory, Richmond*.
- Ang, C. T., Morad, N., Ismail, M. T. and Ismail, N. (2013). Projection of carbon dioxide emissions by energy consumption and transportation in Malaysia: A time series approach. *Journal of Energy Technologies and Policy*, 3: 1 - 10.
- Korre A, Nie Z. and Durucan S. (2010). Life cycle modelling of fossil fuel power generation with post-combustion CO<sub>2</sub> capture. *International Journal of Greenhouse Gas Control* , 4: 289 – 300.
- Samimi, A. and Zarinabadi S. (2012). Reduction of greenhouse gases emission and effect on environment. *Journal of American Science*, 8: 1011 - 1015.
- Mathiesen, B. V., Lund, H. and Karlsson K.. (2011). 100% Renewable energy systems, climate mitigation and economic growth. *Applied Energy*, 88: 488 – 501.
- Ross, J. R. H. (2015). Natural gas reforming and CO<sub>2</sub> mitigation. *Catalysis Today*, 100: 151 –158.
- Braga, T. P., Santos, R. C., Sales, B. M., da Silva, B. R., Pinheiro, A. N., Leite, E. R. and Valentini A. (2014). CO<sub>2</sub> mitigation by carbon nanotube formation during dry reforming of methane analyzed by factorial design combined with response surface methodology. *Chinese Journal of Catalysis*, 35: 514 –523.
- Aasberg-Petersen, K., Dybkjær, I., Ovesen, C. V., Schjødt, N. C., Sehested, J. and Thomsen, S. G. (2011). Natural gas to synthesis gas - catalysts and catalytic processes. *Journal of Natural Gas Science and Engineering*, 3: 423 – 459.
- Verykios, K. E. (2003). Catalytic dry reforming of natural gas for the production of chemicals and hydrogen. *International Journal of Hydrogen Energy*, 28: 1045 – 1063.
- Sharifi, M., Haghighi, M., Rahmani, F. and Karimipour, S. (2014). Syngas production via dry reforming of CH<sub>4</sub> over Co- and Cu-promoted Ni/Al<sub>2</sub>O<sub>3</sub>-ZrO<sub>2</sub> nanocatalysts synthesized via sequential impregnation and sol-gel methods. *Journal of Natural Gas Science and Engineering*, 21: 993 – 1004.
- Ba, K, Oszk, A., Kecsk, T. and Erd A. (2014). Dry reforming of CH<sub>4</sub> on Rh doped Co /Al<sub>2</sub>O<sub>3</sub> catalysts *Catalysis Today*, 228: 123 - 130.
- Ayodele, B. V., Khan, M. R, Lam, S. S. and Cheng, C. K. (2016). Production of CO-rich hydrogen from methane dry reforming over lanthania-supported cobalt catalyst: Kinetic and mechanistic studies. *International Journal of Hydrogen Energy*, 41: 4603 - 4615.
- Khodakov, A. Y, Chu, W. and Fongarland, P. (2007). Advances in the development of novel cobalt Fischer – Tropsch Catalysts for Synthesis of Long-Chain Hydrocarbons and Clean Fuels. *Chemical Reviews*, 107(5): 1692 - 1744.
- Yao, Y., Liu, X., Hildebrandt, D. and Glasser D. (2011). Fischer-Tropsch synthesis using H<sub>2</sub>/CO/CO<sub>2</sub> syngas mixtures over an iron catalyst. *Industrial Engineering Chemical Research*, 50: 11002 –11012.
- Lee, J. H., You, Y. W., Ahn, H. C., Hong, J. S., Kim, S. B., Chang, T. S. and Suh, J. K. (2014). The deactivation study of Co–Ru–Zr catalyst depending on supports in the dry reforming of carbon dioxide. *Journal of Industrial and Engineering Chemistry*, 20: 284 – 289.
- Ruckenstein, E. and Wang, H. Y. (2002). Carbon deposition and catalytic deactivation during CO<sub>2</sub> reforming of CH<sub>4</sub> over Co/ $\gamma$ -Al<sub>2</sub>O<sub>3</sub> catalysts. *Journal of Catalysis*, 205: 289 – 293.
- Zhang, J., Wang, H. and Dalai A. (2007). Development of stable bimetallic catalysts for carbon dioxide reforming of methane. *Journal of Catalysis*, 249: 300 – 310.

20. Corthals, S., Witvrouwen, T., Jacobs, P. and Sels B. (2011). Development of dry reforming catalysts at elevated pressure: D-optimal vs. full factorial design. *Catalysis Today*, 159: 12 – 24.
21. Li, D., Nakagawa, Y. and Tomishige K. (2011). Methane reforming to synthesis gas over Ni catalysts modified with noble metals. *Applied Catalysis A General*, 408: 1 – 24.
22. Özkara-Aydinoğlu, Ş. and Aksoylu, A. E. (2010). CO<sub>2</sub> reforming of methane over Pt–Ni/Al<sub>2</sub>O<sub>3</sub> catalysts: Effects of catalyst composition, and water and oxygen addition to the feed. *International Journal of Hydrogen Energy*, 36: 2950 –2959.
23. Wisniewski, M., Boréave, A. and Gélín P. (2005). Catalytic CO<sub>2</sub> reforming of methane over Ir/Ce<sub>0.9</sub>Gd<sub>0.1</sub>O<sub>2-x</sub>. *Catal Communications*, 6: 596 – 600.
24. Kim, S., Qadir, K., Jin, S., Reddy, A. S., Seo, B., Mun, B. S., Joo, S. H. and Park, J. Y. (2012). Trend of catalytic activity of CO oxidation on Rh and Ru nanoparticles: Role of surface oxide. *Catalysis Today*, 185:131 – 137.
25. Budiman, A.W., Song, S-H., Chang, T-S., Shin, C-H. and Choi M-J. (2012). Dry reforming of methane over cobalt catalysts: A literature review of catalyst development. *Catal Surveys from Asia*, 16: 183 –197.
26. Hadian, N., Rezaei, M., Mosayebi, Z. and Meshkani, F. (2012). CO<sub>2</sub> reforming of methane over nickel catalysts supported on nanocrystalline MgAl<sub>2</sub>O<sub>4</sub> with high surface area. *Journal of Natural Gas Chemistry*, 21: 200 – 206.
27. Sehested, J. (2005). Four challenges for nickel steam-reforming catalysts. *Catalysis Today*, 111: 103 –110.
28. Oliveira, H., Franceschinib, D. and Passos F. (2014). Cobalt catalyst characterization for methane decomposition and carbon nanotube growth. *Journal of Brazilian Chemical Society*, 25: 2339 – 2349.
29. Frontera, P, Macario, A., Aloise, A., Antonucci, P. L., Giordano, G. and Nagy, J. B. (2013). Effect of support surface on methane dry-reforming catalyst preparation. *Catalysis Today*, 218: 18 – 29.
30. Shi, L., Yang, G., Tao, K., Yoneyama, Y., Tan, Y. and Tsubaki N. (2013). An introduction of CO<sub>2</sub> conversion by dry reforming with methane and new route of low-temperature methanol synthesis. *Account of Chemical Research*, 46: 1838 – 1847.
31. Zhang, B., Cai, W., Li, Y., Xu, Y. and Shen W. (2008). Hydrogen production by steam reforming of ethanol over an Ir/CeO<sub>2</sub> catalyst: Reaction mechanism and stability of the catalyst. *International Journal of Hydrogen Energy*, 33: 4377 – 4386.
32. Zhang, B., Tang, X., Li, Y., Cai, W., Xu, Y. and Shen, W. (2006). Steam reforming of bio-ethanol for the production of hydrogen over ceria-supported Co, Ir and Ni catalysts. *Catalysis Communications*, 7: 367 – 372.
33. da Silva, A. M., de Souza, K. R., Mattos, L. V., Jacobs, G., Davis, B. H. and Noronha, F. B. (2011). The effect of support reducibility on the stability of Co/CeO<sub>2</sub> for the oxidative steam reforming of ethanol. *Catalysis Today*, 164: 234 – 239.
34. Luisetto, I, Tuti, S. and Di Bartolomeo E. (2012). Co and Ni supported on CeO<sub>2</sub> as selective bimetallic catalyst for dry reforming of methane. *International Journal of Hydrogen Energy*, 37: 15992 – 15999.
35. Abasaeed, A. E, Al-fatesh, A. S, Naeem, M. A, Ibrahim, A. A. and Fakeeha, A. H. (2015). Catalytic performance of CeO<sub>2</sub> and ZrO<sub>2</sub> supported Co catalysts for hydrogen production via dry reforming of methane. *International Journal of Hydrogen Energy*, 6818 – 6826.
36. Ayodele, B. V., Hossain, M. A., Chong, S. L, Soh, J. C, Abdullah, S., Khan, M. R. and Cheng, C. K. (2016). Non-isothermal kinetics and mechanistic study of thermal decomposition of light rare earth metal nitrate hydrates using thermogravimetric analysis. *Journal of Thermal Analysis and Calorimetry*, 125(1): 423 - 435.
37. Lee, S. S, Zhu, H., Contreras, E. Q, Prakash, A., Puppala, H. L. and Colvin, V. L. (2012). High temperature decomposition of cerium precursors to form ceria nanocrystal libraries for biological applications. *Chemistry Materials*, 24: 424 – 432.
38. Foo, S. Y. (2012). Oxidative dry reforming of methane over alumina-supported Co-Ni catalyst systems. Doctor of Philosophy Thesis, University of New South Wale, Australia.
39. Wang, H, Liu, Y., Wang, L. and Qin, Y. N. (2008). Study on the carbon deposition in steam reforming of ethanol over Co/CeO<sub>2</sub> catalyst. *Chemical Engineering Journal*, 145: 25 – 31.
40. Zeng, S., Fu, Xiaojuan Z., Tiezhuang W. and Xiaoman S. H. (2014). Influence of Fe doping on structure and water oxidation activity of nanocast Co<sub>3</sub>O<sub>4</sub>. *Fuel Process Technology*, 114: 4 – 10.
41. Zeng, S., Zhang, X. Fu, X. Zhang, L. Su, H. and Pan, H. (2012). Co/Ce<sub>x</sub>Zr<sub>1-x</sub>O<sub>2</sub> solid-solution catalysts with cubic fluorite structure for carbon dioxide reforming of methane. *Applied Catalysis B, Environmental*, 136: 308 – 316.

42. Sajjadi, S. M, Haghighi, M. and Rahmani, F. (2014). Dry reforming of greenhouse gases CH<sub>4</sub>/CO<sub>2</sub> over MgO-promoted Ni-Co/Al<sub>2</sub>O<sub>3</sub>-ZrO<sub>2</sub> nanocatalyst: Effect of MgO addition via sol-gel method on catalytic properties and hydrogen yield. *Journal of Sol-Gel Science Technology*, 70(1): 111 –124.
43. San-José-Alonso, D., Juan-Juan, J., Illán-Gómez, M. J. and Román-Martínez, M. C. (2009). Ni, Co and bimetallic Ni-Co catalysts for the dry reforming of methane. *Applied Catalysis A General*, 371: 54 – 59.
44. Zeng, S., Zhang, L., Zhang, X., Wang, Y., Pan, H. and Su, H. (2012). Modification effect of natural mixed rare earths on Co/γ-Al<sub>2</sub>O<sub>3</sub> catalysts for CH<sub>4</sub>/CO<sub>2</sub> reforming to synthesis gas. *International Journal of Hydrogen Energy*, 37: 9994 – 10001.